Published in *Methods*
doi: 10.1016/j.ymeth.2022.08.013

Profiling cell-type specific gene expression in post-mortem human brain samples through laser capture microdissection

Daniel Almeida[1] & Gustavo Turecki*[1,2]

[1] McGill Group for Suicide Studies, Douglas Hospital Research Center, Montreal, QC, Canada, H4H 1R3
[2] Department of Psychiatry, McGill University, Montreal, QC, Canada, H3A 1A1

*Corresponding author: Gustavo.turecki@mcgill.ca

Abstract

The transcriptome of a cell constitutes an essential piece of cellular identity and contributes to the multifaceted complexity and heterogeneity of cell-types within the mammalian brain. Thus, while a wealth of studies have investigated transcriptomic alterations underlying the pathophysiology of diseases of the brain, their use of bulk-tissue homogenates makes it difficult to tease apart whether observed differences are explained by disease state or cellular composition. Cell-type-specific enrichment strategies are, therefore, crucial in the context of gene expression profiling. Laser capture microdissection (LCM) is one such strategy that allows for the capture of specific cell-types, or regions of interest, under microscopic visualization. In this review, we focus on using LCM for cell-type specific gene expression profiling in post-mortem human brain samples. We begin with a discussion of various LCM systems, followed by a walk-through of each step in the LCM to gene expression profiling workflow and a description of some of the limitations associated with LCM. Throughout the review, we highlight important considerations when using LCM with post-mortem human brain samples. Whenever applicable, commercially available kits that have proven successful in the context of LCM with post-mortem human brain samples are described.

Keywords: laser capture microdissection, post-mortem human brain, microscopy, gene expression, RNA-sequencing

Main Text

The transcriptome of a cell constitutes an essential piece of cellular identity and contributes to the multifaceted complexity and heterogeneity of cell-types within the mammalian brain. Recently, single-cell sequencing approaches have revealed that patterns of gene expression in the brain are cell-type specific. Differentiating not only neuronal versus non-neuronal cell-types, but sub-classes within each [1-4]. Thus, while a wealth of studies have investigated transcriptomic alterations underlying the pathophysiology of diseases of the brain, their use of bulk-tissue homogenates makes it difficult to tease apart whether observed differences are explained by changes in gene expression or cellular composition. Importantly, cellular composition may not only vary as a function of disease state, but interindividual differences or technical artefacts related to tissue dissection [5]. Moreover, some disease states are the result of altered gene expression in only a few cell-types. Yet these cell-type specific changes, especially if in rarer populations, are likely to be obscured by tissue heterogeneity. Opposite changes in gene expression across cell-types could, for instance, mask true biological differences in a specific cell-type. As a result, differential expression analyses with bulk-tissue homogenates can produce artefacts that may be attributed to tissue heterogeneity.

Given that cell-type specific enrichment strategies allow for the isolation of a pure population of cells, changes in gene expression can be attributed to disease state as opposed to differences in cellular composition. Laser capture microdissection (LCM), for instance, allows for the capture of specific cell-types under microscopic visualization. The careful capture of these cells ensures that contamination by other cell-types is kept to a minimum. Downstream molecular analyses are, therefore, strongly enriched for a cell-type of interest [6, 7]. The

advantage of LCM over other methods, such as fluorescence-activated nuclei sorting (FANS) or single nuclei RNA-sequencing (snRNA-seq), is that LCM allows for the capture of whole cells. While there is evidence that nuclear transcriptomes faithfully recapitulate the transcriptome of whole cells [4, 8-11], differences in type and proportion of RNA between the cytosol and nucleus do exist [12-15]. It should, however, be noted that this advantage is specific to archived tissue samples, where compromised cellular structure necessitates the isolation of nuclei over whole cells. One final advantage of LCM is that spatial information is preserved. This information is especially important in regions, such as the prefrontal cortex, with clear cytoarchitectural organization. Using morphologically defined boundaries, LCM allows for the capture of cells from specific cortical layers. Cortical pyramidal neurons, for instance, exist in both supra- and infragranular layers. Importantly, these neurons not only vary in morphology and size, but the regions that they project to [16-21]. Given these differences, it is unsurprising that a disease state would associate with layer-specific alterations to the transcriptome of these neurons [22].

While LCM is typically used to isolate hundreds of cells, this approach has been shown to be effective in the isolation and downstream molecular profiling of single cells [7]. Beyond the isolation of a specific cell-type, LCM has also been successfully used to dissect and isolate cytoarchitecturally or neurochemically defined sub-regions within a tissue section [6, 23-28], as well as pathological lesions and microvessels from human brain samples [29, 30]. In this review, we focus on profiling cell-type specific gene expression in post-mortem human brain samples through LCM. We, first, begin with a description of LCM and then proceed into discussing variations in each step of the LCM workflow, from tissue preservation to downstream gene expression profiling via PCR, microarrays and RNA-seq (Figure 1). Throughout the review, we

highlight challenges and solutions that others have reported while using LCM with post-mortem human brain samples. Table 1 lists each of the studies cited within this review and the aforementioned variations in each step of the LCM workflow. Additionally, we highlight some of most commonly used and commercially available kits, whenever applicable.

1. Laser Capture Microdissection Systems

There are two general types of LCM systems: infrared (IR) capture systems and ultraviolet (UV) cutting systems. The principle components of microdissection technology includes the (i) visualization of cells or regions of interest via microscopy, (ii) transfer of laser energy that results in the formation of a polymer-cell composite (IR capture method) or photoablation of cells surrounding a selected area (UV cutting method), and (iii) the removal of cells or regions of interest from the tissue section [31]. While the first commercial version of LCM, developed by Arcturus, used a very low power IR laser to activate a thermoplastic film and capture a cell-type of interest, UV cutting systems use a high power laser to burn through tissue during dissection. Given that UV light can damage DNA, RNA, and proteins, this approach may be better suited for isolating larger structures within tissue sections than individual cells [31]. Nonetheless, LCM is typically used to describe either IR capture or UV cutting. LCM systems that are capable of both IR capture and UV cutting, allow for the combined use of both lasers. One application of this combined technology would be the use of the UV laser to cut around a cell-type of interest prior to IR capture. This approach may be especially necessary when a cell-type of interest is in close proximity to other cells and has been shown to improve capture quality [32].

Newer LCM systems have also modified the method through which cells are collected. For instance, the Zeiss PALM MicroBeam LCM system employs laser pressure catapulting

technology to retrieve the microdissected sample into the cap of a tube overlayed on top of the tissue being dissected. Briefly, a focused UV laser beam is used to cut the tissue sample, while a defocused laser beam is used to lift the dissected sampled into the cap of the collection tube. One advantage to this type of contact-free technology is that it minimizes the risk of contamination [33]. The Leica LMD6 and LMD7 microscopes also use a focused UV laser beam to microdissect the tissue sample, but since an upright microscope is used, the collection of the sample happens solely by gravity into a tube placed below the tissue section (i.e., contact-free gravity-assisted microdissection) [33]. The difference between the LMD6 and LMD7 systems is that the later allows for a higher laser power. The LMD6 system is, therefore, most suitable for the dissection of soft tissues such as brain, liver or kidney. LMD7 is, on the other hand, compatible with any tissue-type.

2. Tissue preservation and quality

LCM has been applied to post-mortem brain samples preserved through a wide range of techniques, including fresh frozen, formalin-fixed (FF) or formalin-fixed paraffin-embedded (FFPE). The ideal tissue preservation technique ensures that both tissue morphology and RNA integrity are preserved. Fresh frozen tissue offers excellent preservation of RNA, but freezing and cryostat sectioning can significantly disrupt tissue morphology. Formalin-fixed or FFPE tissues, on the other hand, preserve tissue morphology, but create cross-links between nucleic acids and proteins that interfere with the RNA recovery. RNA extracted from FFPE tissues is, therefore, usually degraded [34-37]. Other considerations include post-mortem interval, tissue pH, and the agonal state of the decedent, which have all been shown to effect downstream gene expression based analyses [36, 38-41].

3. Tissue sectioning

The optimal tissue section thickness for LCM is between 5–15 μm, with tissue sections thinner than 5 μm not capturing entire cell thickness. Thinner sections may also lead to the loss of specific cell-types during sectioning [32]. Tissue sections thicker than 15 μm may not microdissect completely, thereby resulting in reduced capture efficiency [42, 43]. Once sectioned on a cryostat or microtome, the slide that a section is mounted on depends on the type of LCM instrument to be used. For IR-based systems, sections should be mounted onto uncharged and uncoated glass slides [31, 44]. For UV-based systems, sections should be mounted onto polyethylene napthalate (PEN) or polyethylene tetraphthalate (PET) membrane slides [31]. Membrane slides are also compatible with LCM systems that are capable of both IR capture and UV cutting. Sections should then be immediately stored at -80°C and transported temporarily on dry ice to avoid thawing of the tissue sample. Freeze/thaw cycles should be avoided as they are detrimental to RNA quality [45].

4. Staining

LCM has been used to procure a variety of cell-types within the human brain. Given that microscopic visualization is fundamental to the technique, staining approaches vary by cell-type of interest. In some cases, a specific cell-type can be easily identified by size, morphology or natural pigmentation. For instance, pyramidal neurons, noradrenergic neurons, Von Economo neurons and Purkinje cells, can all been captured by LCM using a standard cresyl violet or commercially available HistoGene stain (Thermo Fisher Scientific, MA, USA). Cell-types that can only be accurately identified by the presence of specific markers require staining via

immunohistochemistry or *in situ* hybridization (ISH). Irrespective of the method used, maintaining RNA integrity during the LCM process is crucial. To combat this issue, an RNAse inhibitor can be added to the staining solution. Other forms of RNA stabilization also exist and have included performing LCM under an argon atmosphere and using a concentrated solution of ethanol to enhance the fixation and dehydration of tissue samples [46].

4.1. Simple stains

When identifying cells by size, morphology or natural pigmentation, the HistoGene staining solution, developed by Arcturus, has often been used. The HistoGene stain is a fast-penetrating stain that provides good contrast between nuclei and cytoplasm. The solution can be purchased as part of a kit that also includes uncharged glass slides, high concentration ethanol, xylene and staining jars. However, the solution itself can also be purchased separately at a fraction of the cost. In fact, the use of the kit appears unnecessary as the solution can be combined with regular reagent grade ethanol and xylene [7]. The entire staining process is short and has minimal effect on RNA integrity [32]. Importantly, previous investigations have shown that the HistoGene stain, as well as a standard cresyl violet stain, is sufficient for the identification and capture of some cell-types. For instance, in a study by Ordway and colleagues, the authors used the HistoGene stain to identify noradrenergic neurons in the locus coeruleus [32]. Noradrenergic neurons were distinguishable from other cell-types within the locus coeruleus by their neuromelanin content and, therefore, dark appearance [32, 47]. A similar approach has also been used to identify and capture dopaminergic neurons in the substantia nigra pars compacta and ventral tegmental area [7, 48]. Oligodendrocytes, on the other hand, can be identified by the dark staining of their compact nucleus, which is in contrast to the light staining

observed with astrocytes and microglia [32, 49]. Other cell-types such as pyramidal neurons, Von Economo neurons and Purkinje cells are easily identifiable by their unique morphology and regional distribution. Pyramidal neurons have a distinct pyramidal shape and large apical dendrite [50, 51]. In the cortex, pyramidal neurons are located in supragranular (II – III) and infragranlular (V – VI) layers. Layer I, on the other hand, is characterized by a relatively homogenous population of GABAergic neurons that can easily be identified and captured via LCM [51]. In general, the laminar organization of cortical neurons results in distinct physiological properties and transcriptional profiles [52]. It is, therefore, crucial that cortical layer be considered in molecular analyses. LCM has proved to be useful in this respect and has aided in the characterization of layer-specific transcriptional profiles in both health and disease [22, 27, 51, 53-56]. Other more region-specific cell-types have also been interrogated by LCM. For instance, von Economo neurons (VENs) are a type of specialized bipolar projection neuron that are primarily distributed in layer V of the anterior cingulate cortex and frontoinsular cortex [57, 58]. These cells are identifiable by their large size, characteristic spindle-shaped soma and thick dendrites [58, 59]. Indeed, the average volume of VENs is about 4.6 times larger than that of infragranular pyramidal neurons [58]. By way of LCM coupled with RNA-seq, the transcriptional landscape of VENs in the anterior cingulate cortex has previously been characterized [60]. In this investigation, the authors utilized a cresyl violet stain to identify and capture VENs [60]. A final region-specific cell-type previously explored via LCM is the Purkinje cell located in the cerebellum. Similar to the aforementioned cell-types, a cresyl violet stain is sufficient to identify and capture Purkinje cells [61].

4.2. Immunohistochemistry

In cases where a cell-type is not easily identifiable by size, morphology or natural pigmentation, other staining approaches are required. The most common of which has been some variation of a rapid immunohistochemistry based protocol. While these protocols tend to be longer in duration than a HistoGene or cresyl violet based stain, average RNA quality and downstream sequencing metrics have been shown to be comparable [7, 32]. For instance, in a study comparing dopaminergic neurons stained via HistoGene versus a TH (tyrosine hydroxylase) antibody, the authors found similar mapping rates in RNA-seq [7]. One caveat, however, was that the number of identified genes was greater with the HistoGene stain, which may be explained by differences in RNA degradation. In addition to this, the authors also investigated the impacts of staining time on mapping rate and number of detected genes. While increasing the primary TH antibody staining time from 4 minutes to 20 and 60 minutes resulted in a slight decrease in the average mapping rate, the number of detected genes were comparable, as was the expression of dopaminergic marker genes. Other sub-classes of neurons have also been identified by immunohistochemistry and captured by LCM, including, parvalbumin positive interneurons in the temporal cortex [62] and TH positive serotonergic neurons in the dorsal raphe [63].

Immunohistochemistry has also been used to visualize and capture glial cells for downstream expression based analyses. The visualization of astrocytes, for instance, typically involves staining for GFAP (glial fibrillary acidic protein) [32, 36, 64-67]. This approach is preferred over a cresyl violet stain, since identification based solely on size seems to result in contamination by GABAergic interneurons [68]. Like astrocytes, oligodendrocytes have been visualized and captured using both a cresyl violet and immunohistochemistry based approach

[32, 64, 69-71]. In the latter case, oligodendrocytes have been stained with antibodies against OSP (oligodendrocyte specific protein) [71, 72] and CNP (2',3'-Cyclic Nucleotide 3' Phosphodiesterase) [64, 70]. Microglia can be identified by CD68 (cluster of Differentiation 68) [71, 73] and LN3 staining (anti-HLA-DR), with the latter being used as a marker of activated microglia [74]. Finally, microvessel endothelial cells have been isolated via LCM by staining against von Willebrand factor [75] or collagen IV [67], as well as with the fluorescein-labeled lectin UEA I (ulex europeaus agglutinin I) [29].

4.3. Fluorescent in situ hybridization

Recent advances in fluorescent *in situ* hybridization (FISH) [9] have made it a reliable method for labeling specific cell-types for LCM. A major advantage of FISH is the increased capacity for multi-labelling. This is especially important in the context of isolating cell-types that are molecularly rather than morphologically defined. Despite this major advantage, human brain tissue is characterized by high levels of autofluorescence from lipofuscin. However, this issue has been previously circumvented via the application of an optical filter [76]. The creation of the RNAscope technology (Advanced Cell Diagnostics, CA, USA) has also aided in the application of FISH to LCM. The RNAscope probe design strategy and hybridization-based signal amplification system allows for single-molecule visualization by the simultaneous amplification of signal and suppression of background noise [77]. The application of RNAscope technology with LCM may allow for the isolation of a wider range of molecularly distinct sub-classes of cells. Indeed, this approach has been used to capture SLC17A7 (vesicular glutamate transporter 1) expressing glutamatergic cells and SST (somatostatin) expressing GABAergic cells via LCM [76].

5. Microdissection

There are many factors that can affect the microdissection process and quality of downstream molecular analyses. One factor that can have a determinantal impact on capture efficiency, for instance, is humidity. In a study by Ordway and colleagues, capture efficiency was approximately 80% at a relative humidity of 20 to 33%, but dropped to approximately 40% at a humidity of 41%. Humidity also influenced RNA integrity in a time-dependent manner at or above a relative humidity of 33% [32]. The effects of humidity, however, likely depend on several factors, including the capture system being employed.

LCM systems allow users to adjust the physical parameters of the laser. Importantly, these parameters will vary depending on the size and type of cell being captured, as well as the proximity of nearby cells. Both pulse power and duration have a direct impact on capture spot size. If pulse settings are set too low, the corresponding capture spot size will not be large enough to capture whole cells. The optimal capture spot size will, ultimately, vary depending by the cell-type of interest and should be experimentally determined. For instance, neurons may require higher pulse settings than glia, even when captured from the same tissue section [32]. Once an optimal capture spot size is found, pulse power and duration may need to be adjusted for each capture. Maintaining a constant pulse setting, for instance, has been shown to vary capture spot size across captures. Deviating from the optimal capture spot size can result in reduced capture efficiency and increased rates of contamination from nearby cells [32].

While the number of cells captured varies from study to study, the range is typically between 100 to 500 cells [7, 32, 50, 62, 76]. Ultimately, the number of captured cells should be balanced between having enough material for downstream molecular analyses and time.

Capturing fewer than 100 cells may result in a failure to detect lowly expressed genes, while capturing greater than 500 cells can be time-consuming. This latter point is especially important as LCM capture time has been shown to significantly affect downstream molecular analyses and should be kept to a minimum [36, 44]. In general, total capture time should not exceed more than 1 hour.

6. RNA extraction and amplification

LCM has been combined with a wide array of molecular techniques for studying gene expression, such as PCR, microarrays and RNA-seq. In most previously published reports using LCM with post-mortem human brain samples, RNA was first extracted (Table 1). However, direct lysis of microdissected material, without RNA extraction, has been shown to be effective when synthesizing cDNA via oligo(dT) priming [7, 60]. Importantly, while microdissected samples are stored at −80°C, the length of time between LCM and RNA extraction should be kept to a minimum [36].

The two most common ways of extracting RNA from microdissected samples has been with the PicoPure RNA Isolation kit (Thermo Fisher Scientific, MA, USA) developed by Arcturus [23, 24, 26, 27, 44, 48, 50, 56, 61, 63, 66-72, 76], the RNAqueous system (Thermo Fisher Scientific, MA, USA) developed by Ambion [32, 36, 47, 53, 54, 64], and the RNeasy Micro kit (Qiagen, MD, USA) developed by Qiagen [6, 22, 30, 51, 74]. Each kit is capable of isolating RNA from a small number of captured cells. While DNAse treatment is optional, it is highly recommended that this step be performed.

Due to the limited number of cells that can be captured by LCM, RNA yields may be low. To address this issue, amplification methods have been developed. In the case of

microarrays, the most commonly used amplification method has involved the *in vitro* transcription (IVT) of a cDNA template into antisense RNA (aRNA). RiboAmp kits (Thermo Fisher Scientific, MA, USA), for instance, utilize this approach to amplify RNA from as little as 100 to 500 pg of total RNA or as few as 10 to 50 cells captured by LCM. Tecan's Ovation amplification system (Tecan, Männedorf, Switzerland), in contrast, takes advantage of single primer isothermal amplification (SPIA) technology to amplify single stranded cDNA. Importantly, commercial kits based on IVT versus SPIA technology have been compared [78]. IVT-based amplification kits require numerous steps and are therefore time-consuming and labour-intensive. SPIA-based amplification kits involve fewer steps and avoid RNA handling during the amplification process [78]. Most recently, SMART (Switching Mechanism at the 5′ end of RNA Template) PCR (Takara Bio, CA, USA) has also been used to amplify material from LCM samples [7]. SMART technology leverages the template-switching capability of certain reverse transcriptases to capture full-length sequence information from RNA during cDNA synthesis [79-82]. cDNA is then pre-amplified via PCR and can be used to generate RNA-seq libraries from as little as a few picograms of RNA [79, 80]. While IVT- and PCR-based amplification have been compared, findings have been mixed [83, 84].

7. Analyzing gene expression

An important step in the LCM workflow is the confirmation of capture quality. By way of qPCR, the expression of marker genes can be used to determine whether a population of captured cells is relatively homogenous or contaminated by other cell-types [29, 30, 32, 48, 51, 76]. While the expression of these genes can also be determined through microarrays or RNA-seq, qPCR is a relatively simple and inexpensive way of confirming capture quality. Beyond this,

LCM qPCR has also been employed to investigate hypothesis-driven differences in gene expression [27, 30, 47, 51, 56, 62-64, 72, 76] and to validate results generated from RNA-seq or microarrays [22-24, 50, 62, 66, 71]. In the latter case, an aliquot of cDNA can sometimes be saved for qPCR.

Historically, microarrays have been the most commonly used method for profiling global patterns of gene expression in LCM samples. RNA-seq, which offers several advantages over microarrays, has only recently been applied in this context [85]. Of the few published reports on post-mortem LCM RNA-seq, cDNA synthesis and amplification has commonly been carried out via SMART PCR [7, 48, 69]. Notably, this technology is commercially available through Takara's suite of RNA-seq library construction kits. Amongst the suite of kits are those that use either oligo(dT) or random priming to generate cDNA. Takara's SMART-Seq v4 kit, for instance, utilizes oligo(dT) priming and SMART-PCR to generate high-quality, full-length cDNA directly from cells or 10 pg–10 ng of total RNA. The PLUS version of the kit includes a library construction component that incorporates enzymatic fragmentation and stem-loop adapters to construct Illumina-compatible RNA-seq libraries. The SMARTer Stranded Total RNA-Seq kit v3, in contrast, uses random priming followed by the addition of Illumina adaptors (Illumina, CA, USA) with barcodes and cleavage of ribosomal cDNA to generate RNA-seq libraries. A major difference between the two approaches is that the former kit is recommended for high quality RNA samples with a RIN $\geq$ 8, while the latter is suitable for degraded samples. One additional benefit of the SMARTer Stranded Total RNA-seq kit v3 is its inclusion of unique molecular identifiers for the identification and correction of PCR biases. A random priming based approach may, however, be more sensitive to genomic contamination. Importantly, both oligo(dT) [7, 60] and random priming [6, 69] have been used to synthesize cDNA from LCM

samples for RNA-seq. In a report by Nichterwitz et al. (2016), cDNA was generated from both captured cells and extracted RNA through oligo(dT) priming. RNA-seq libraries were then synthesized using transposase-based tagmentation and the simultaneous ligation of Illumina sequencing adaptors. Interestingly, direct lysis of captured cells produced greater cDNA yields than extracted RNA (Nichterwitz et al., 2016). In a report by Piras et al. (2020), RNA-seq libraries were constructed from RNA using an earlier version of the SMARTer Stranded Total RNA-seq kit. Other commercially available kits, including Tecan's Ovation RNA-seq System v2 kit, utilize a combination of oligo(dT) and random priming to synthesize cDNA. While this kit is most compatible with high quality RNA samples, it has been previously used with RNA extracted from captured microglia [74].

8. Limitations

While there are a number of advantages to using LCM with post-mortem human brain tissue, there are also disadvantages that should be considered. For one, LCM is a low-throughput technique for isolating a population of cells. Total time, from staining to microdissection, will vary depending on the length of the staining protocol and the rarity of the cellular population being microdissected. In general, the entire process, from staining to microdissection, can take up to 1–1.5 hours when using a simple staining procedure [44]. However, in cases where a cell-type is only identifiable via the presence of a specific marker, staining procedures alone can take up to 1–2.5 hours in duration [7, 76]. Another problem that can be encountered with LCM is poor capture efficiency. This issue is usually a result of incomplete tissue dehydration or a pulse setting that is too low for complete permeation of the melted polymer onto the section. Related to the issue of capture efficiency is the balance between capturing entire cells and their processes,

while minimizing contamination from neighbouring cells. Importantly, this issue may be particularly relevant for specific cell-types. Neurons, for instance, are usually larger in diameter and, therefore, require a larger capture spot size than glia. Yet, neurons are also typically in close proximity to glia. A larger capture spot size may, therefore, increase the likelihood of capturing unwanted neighbouring cells. One solution may be to use a UV laser to cut around a cell-type of interest prior to IR capture. Importantly, this approach has been shown to result in the successful capture of noradrenergic neurons from the human locus coeruleus [32]. Finally, while LCM has been shown to be effective in the isolation and downstream gene expression profiling of single cells [7], its low-throughout nature makes it an inefficient strategy for capturing enough cells for single-cell analyses. Instead, the unique feature of LCM is that is allows for the precise capture of specific cells under microscopic visualization. LCM is, therefore, ideally suited for hypothesis-driven research related to a specific cell-type of interest.

9. Conclusions and future directions

In sum, LCM is a reliable tool for capturing a wide array of cell-types from post-mortem human brain tissue. Significant advancements at all stages of the LCM workflow have increased the feasibility of using this tool with challenging tissue samples. These advancements have allowed researchers to collect reliable expression data from depreciating numbers of cells. As a consequence, even rare cell-types are now open to investigation. This is crucial given new insights garnered from single-cell sequencing on molecularly defined cell-types within the human brain. Future work, however, is needed to systematically compare the most commonly used approaches for profiling gene expression in LCM samples.

Funding

GT holds a Canada Research Chair (Tier 1) and is supported by grants from the Canadian Institute of Health Research (CIHR) (FDN148374 and ENP161427 (ERA-NET ERA PerMed)). DA is a Vanier Scholar funded by the Canadian Institute of Health Research (CIHR).

Competing Interests

The authors declare no conflict of interest.

References

[1] B.B. Lake, S. Chen, B.C. Sos, J. Fan, G.E. Kaeser, Y.C. Yung, T.E. Duong, D. Gao, J. Chun, P.V. Kharchenko, K. Zhang, Integrative single-cell analysis of transcriptional and epigenetic states in the human adult brain, Nat Biotechnol 36(1) (2018) 70-80.

[2] N. Habib, I. Avraham-Davidi, A. Basu, T. Burks, K. Shekhar, M. Hofree, S.R. Choudhury, F. Aguet, E. Gelfand, K. Ardlie, D.A. Weitz, O. Rozenblatt-Rosen, F. Zhang, A. Regev, Massively parallel single-nucleus RNA-seq with DroNc-seq, Nat Methods 14(10) (2017) 955-958.

[3] C. Nagy, M. Maitra, A. Tanti, M. Suderman, J.F. Theroux, M.A. Davoli, K. Perlman, V. Yerko, Y.C. Wang, S.J. Tripathy, P. Pavlidis, N. Mechawar, J. Ragoussis, G. Turecki, Single-nucleus transcriptomics of the prefrontal cortex in major depressive disorder implicates oligodendrocyte precursor cells and excitatory neurons, Nat Neurosci (2020).

[4] B.B. Lake, R. Ai, G.E. Kaeser, N.S. Salathia, Y.C. Yung, R. Liu, A. Wildberg, D. Gao, H.L. Fung, S. Chen, R. Vijayaraghavan, J. Wong, A. Chen, X. Sheng, F. Kaper, R. Shen, M. Ronaghi, J.B. Fan, W. Wang, J. Chun, K. Zhang, Neuronal subtypes and diversity revealed by single-nucleus RNA sequencing of the human brain, Science 352(6293) (2016) 1586-90.

[5] U. Isildak, M. Somel, J.M. Thornton, H.M. Donertas, Temporal changes in the gene expression heterogeneity during brain development and aging, Sci Rep 10(1) (2020) 4080.

[6] A.E. Jaffe, D.J. Hoeppner, T. Saito, L. Blanpain, J. Ukaigwe, E.E. Burke, L. Collado-Torres, R. Tao, K. Tajinda, K.R. Maynard, M.N. Tran, K. Martinowich, A. Deep-Soboslay, J.H. Shin, J.E. Kleinman, D.R. Weinberger, M. Matsumoto, T.M. Hyde, Profiling gene expression in the human dentate gyrus granule cell layer reveals insights into schizophrenia and its genetic risk, Nat Neurosci 23(4) (2020) 510-519.

[7] S. Nichterwitz, G. Chen, J. Aguila Benitez, M. Yilmaz, H. Storvall, M. Cao, R. Sandberg, Q. Deng, E. Hedlund, Laser capture microscopy coupled with Smart-seq2 for precise spatial transcriptomic profiling, Nat Commun 7 (2016) 12139.

[8] N. Habib, Y. Li, M. Heidenreich, L. Swiech, I. Avraham-Davidi, J.J. Trombetta, C. Hession, F. Zhang, A. Regev, Div-Seq: Single-nucleus RNA-Seq reveals dynamics of rare adult newborn neurons, Science 353(6302) (2016) 925-8.

[9] R.V. Grindberg, J.L. Yee-Greenbaum, M.J. McConnell, M. Novotny, A.L. O'Shaughnessy, G.M. Lambert, M.J. Arauzo-Bravo, J. Lee, M. Fishman, G.E. Robbins, X. Lin, P. Venepally, J.H. Badger, D.W. Galbraith, F.H. Gage, R.S. Lasken, RNA-sequencing from single nuclei, Proc Natl Acad Sci U S A 110(49) (2013) 19802-7.

[10] S.R. Krishnaswami, R.V. Grindberg, M. Novotny, P. Venepally, B. Lacar, K. Bhutani, S.B. Linker, S. Pham, J.A. Erwin, J.A. Miller, R. Hodge, J.K. McCarthy, M. Kelder, J. McCorrison, B.D. Aevermann, F.D. Fuertes, R.H. Scheuermann, J. Lee, E.S. Lein, N. Schork, M.J. McConnell, F.H. Gage, R.S. Lasken, Using single nuclei for RNA-seq to capture the transcriptome of postmortem neurons, Nat Protoc 11(3) (2016) 499-524.

[11] W. Zeng, S. Jiang, X. Kong, N. El-Ali, A.R. Ball, Jr., C.I. Ma, N. Hashimoto, K. Yokomori, A. Mortazavi, Single-nucleus RNA-seq of differentiating human myoblasts reveals the extent of fate heterogeneity, Nucleic Acids Res 44(21) (2016) e158.

[12] R.A. Barthelson, G.M. Lambert, C. Vanier, R.M. Lynch, D.W. Galbraith, Comparison of the contributions of the nuclear and cytoplasmic compartments to global gene expression in human cells, BMC Genomics 8 (2007) 340.

[13] K. Bahar Halpern, I. Caspi, D. Lemze, M. Levy, S. Landen, E. Elinav, I. Ulitsky, S. Itzkovitz, Nuclear Retention of mRNA in Mammalian Tissues, Cell Rep 13(12) (2015) 2653-62.

[14] B.B. Lake, S. Codeluppi, Y.C. Yung, D. Gao, J. Chun, P.V. Kharchenko, S. Linnarsson, K. Zhang, A comparative strategy for single-nucleus and single-cell transcriptomes confirms accuracy in predicted cell-type expression from nuclear RNA, Sci Rep 7(1) (2017) 6031.

[15] N. Thrupp, C. Sala Frigerio, L. Wolfs, N.G. Skene, N. Fattorelli, S. Poovathingal, Y. Fourne, P.M. Matthews, T. Theys, R. Mancuso, B. de Strooper, M. Fiers, Single-Nucleus RNA-Seq Is Not Suitable for Detection of Microglial Activation Genes in Humans, Cell Rep 32(13) (2020) 108189.

[16] Y. Kubota, S. Hatada, S. Kondo, F. Karube, Y. Kawaguchi, Neocortical inhibitory terminals innervate dendritic spines targeted by thalamocortical afferents, J Neurosci 27(5) (2007) 1139-50.

[17] S.J. Cruikshank, O.J. Ahmed, T.R. Stevens, S.L. Patrick, A.N. Gonzalez, M. Elmaleh, B.W. Connors, Thalamic control of layer 1 circuits in prefrontal cortex, J Neurosci 32(49) (2012) 17813-23.

[18] Y. Hirai, M. Morishima, F. Karube, Y. Kawaguchi, Specialized cortical subnetworks differentially connect frontal cortex to parahippocampal areas, J Neurosci 32(5) (2012) 1898-913.

[19] N.C. Dembrow, R.A. Chitwood, D. Johnston, Projection-specific neuromodulation of medial prefrontal cortex neurons, J Neurosci 30(50) (2010) 16922-37.

[20] Y. Ueta, Y. Hirai, T. Otsuka, Y. Kawaguchi, Direction- and distance-dependent interareal connectivity of pyramidal cell subpopulations in the rat frontal cortex, Front Neural Circuits 7 (2013) 164.

[21] P.L. Gabbott, T.A. Warner, P.R. Jays, P. Salway, S.J. Busby, Prefrontal cortex in the rat: projections to subcortical autonomic, motor, and limbic centers, J Comp Neurol 492(2) (2005) 145-77.

[22] D. Arion, J.P. Corradi, S. Tang, D. Datta, F. Boothe, A. He, A.M. Cacace, R. Zaczek, C.F. Albright, G. Tseng, D.A. Lewis, Distinctive transcriptome alterations of prefrontal pyramidal neurons in schizophrenia and schizoaffective disorder, Mol Psychiatry 20(11) (2015) 1397-405.

[23] I.A. Kerman, R. Bernard, W.E. Bunney, E.G. Jones, A.F. Schatzberg, R.M. Myers, J.D. Barchas, H. Akil, S.J. Watson, R.C. Thompson, Evidence for transcriptional factor dysregulation in the dorsal raphe nucleus of patients with major depressive disorder, Front Neurosci 6 (2012) 135.

[24] R. Bernard, I.A. Kerman, F. Meng, S.J. Evans, I. Amrein, E.G. Jones, W.E. Bunney, H. Akil, S.J. Watson, R.C. Thompson, Gene expression profiling of neurochemically defined regions of the human brain by in situ hybridization-guided laser capture microdissection, J Neurosci Methods 178(1) (2009) 46-54.

[25] R. Bernard, S. Burke, I.A. Kerman, Region-specific in situ hybridization-guided laser-capture microdissection on postmortem human brain tissue coupled with gene expression quantification, Methods Mol Biol 755 (2011) 345-61.

[26] A. Medina, S.J. Watson, W. Bunney, Jr., R.M. Myers, A. Schatzberg, J. Barchas, H. Akil, R.C. Thompson, Evidence for alterations of the glial syncytial function in major depressive disorder, J Psychiatr Res 72 (2016) 15-21.

[27] P. Katsel, W. Byne, P. Roussos, W. Tan, L. Siever, V. Haroutunian, Astrocyte and glutamate markers in the superficial, deep, and white matter layers of the anterior cingulate gyrus in schizophrenia, Neuropsychopharmacology 36(6) (2011) 1171-7.

[28] Z. He, D. Han, O. Efimova, P. Guijarro, Q. Yu, A. Oleksiak, S. Jiang, K. Anokhin, B. Velichkovsky, S. Grunewald, P. Khaitovich, Comprehensive transcriptome analysis of neocortical layers in humans, chimpanzees and macaques, Nat Neurosci 20(6) (2017) 886-895.

[29] J. Mojsilovic-Petrovic, M. Nesic, A. Pen, W. Zhang, D. Stanimirovic, Development of rapid staining protocols for laser-capture microdissection of brain vessels from human and rat coupled to gene expression analyses, J Neurosci Methods 133(1-2) (2004) 39-48.

[30] M. Slevin, J. Krupinski, N. Rovira, M. Turu, A. Luque, M. Baldellou, C. Sanfeliu, N. de Vera, L. Badimon, Identification of pro-angiogenic markers in blood vessels from stroked-affected brain tissue using laser-capture microdissection, BMC Genomics 10 (2009) 113.

[31] V. Espina, J.D. Wulfkuhle, V.S. Calvert, A. VanMeter, W. Zhou, G. Coukos, D.H. Geho, E.F. Petricoin, 3rd, L.A. Liotta, Laser-capture microdissection, Nat Protoc 1(2) (2006) 586-603.

[32] G.A. Ordway, A. Szebeni, M.M. Duffourc, S. Dessus-Babus, K. Szebeni, Gene expression analyses of neurons, astrocytes, and oligodendrocytes isolated by laser capture microdissection from human brain: detrimental effects of laboratory humidity, J Neurosci Res 87(11) (2009) 2430-8.

[33] P. Pinzani, C. Orlando, M. Pazzagli, Laser-assisted microdissection for real-time PCR sample preparation, Mol Aspects Med 27(2-3) (2006) 140-59.

[34] A. Esteve-Codina, O. Arpi, M. Martinez-Garcia, E. Pineda, M. Mallo, M. Gut, C. Carrato, A. Rovira, R. Lopez, A. Tortosa, M. Dabad, S. Del Barco, S. Heath, S. Bague, T. Ribalta, F. Alameda, N. de la Iglesia, C. Balana, G. Group, A Comparison of RNA-Seq Results from Paired Formalin-Fixed Paraffin-Embedded and Fresh-Frozen Glioblastoma Tissue Samples, PLoS One 12(1) (2017) e0170632.

[35] I. Wimmer, A.R. Troscher, F. Brunner, S.J. Rubino, C.G. Bien, H.L. Weiner, H. Lassmann, J. Bauer, Systematic evaluation of RNA quality, microarray data reliability and pathway analysis in fresh, fresh frozen and formalin-fixed paraffin-embedded tissue samples, Sci Rep 8(1) (2018) 6351.

[36] L. Tagliafierro, K. Bonawitz, O.C. Glenn, O. Chiba-Falek, Gene Expression Analysis of Neurons and Astrocytes Isolated by Laser Capture Microdissection from Frozen Human Brain Tissues, Front Mol Neurosci 9 (2016) 72.

[37] R. Jiang, R.S. Scott, L.M. Hutt-Fletcher, Laser capture microdissection for analysis of gene expression in formalin-fixed paraffin-embedded tissue, Methods Mol Biol 755 (2011) 77-84.

[38] M. Atz, D. Walsh, P. Cartagena, J. Li, S. Evans, P. Choudary, K. Overman, R. Stein, H. Tomita, S. Potkin, R. Myers, S.J. Watson, E.G. Jones, H. Akil, W.E. Bunney, Jr., M.P. Vawter, C. Members of National Institute of Mental Health Conte, C. Pritzker Neuropsychiatric Disorders Research, Methodological considerations for gene expression profiling of human brain, J Neurosci Methods 163(2) (2007) 295-309.

[39] J.Z. Li, M.P. Vawter, D.M. Walsh, H. Tomita, S.J. Evans, P.V. Choudary, J.F. Lopez, A. Avelar, V. Shokoohi, T. Chung, O. Mesarwi, E.G. Jones, S.J. Watson, H. Akil, W.E. Bunney, Jr.,

R.M. Myers, Systematic changes in gene expression in postmortem human brains associated with tissue pH and terminal medical conditions, Hum Mol Genet 13(6) (2004) 609-16.

[40] H. Tomita, M.P. Vawter, D.M. Walsh, S.J. Evans, P.V. Choudary, J. Li, K.M. Overman, M.E. Atz, R.M. Myers, E.G. Jones, S.J. Watson, H. Akil, W.E. Bunney, Jr., Effect of agonal and postmortem factors on gene expression profile: quality control in microarray analyses of postmortem human brain, Biol Psychiatry 55(4) (2004) 346-52.

[41] K. White, P. Yang, L. Li, A. Farshori, A.E. Medina, H.R. Zielke, Effect of Postmortem Interval and Years in Storage on RNA Quality of Tissue at a Repository of the NIH NeuroBioBank, Biopreserv Biobank 16(2) (2018) 148-157.

[42] V. Espina, J. Milia, G. Wu, S. Cowherd, L.A. Liotta, Laser capture microdissection, Methods Mol Biol 319 (2006) 213-29.

[43] C. Bevilacqua, S. Makhzami, J.C. Helbling, P. Defrenaix, P. Martin, Maintaining RNA integrity in a homogeneous population of mammary epithelial cells isolated by Laser Capture Microdissection, BMC Cell Biol 11 (2010) 95.

[44] C.Y. Pietersen, M.P. Lim, T.U. Woo, Obtaining high quality RNA from single cell populations in human postmortem brain tissue, J Vis Exp (30) (2009).

[45] J. Botling, K. Edlund, U. Segersten, S. Tahmasebpoor, M. Engstrom, M. Sundstrom, P.U. Malmstrom, P. Micke, Impact of thawing on RNA integrity and gene expression analysis in fresh frozen tissue, Diagn Mol Pathol 18(1) (2009) 44-52.

[46] M. Clement-Ziza, A. Munnich, S. Lyonnet, F. Jaubert, C. Besmond, Stabilization of RNA during laser capture microdissection by performing experiments under argon atmosphere or using ethanol as a solvent in staining solutions, RNA 14(12) (2008) 2698-704.

[47] M.J. Chandley, A. Szebeni, K. Szebeni, J.D. Crawford, C.A. Stockmeier, G. Turecki, R.M. Kostrzewa, G.A. Ordway, Elevated gene expression of glutamate receptors in noradrenergic neurons from the locus coeruleus in major depression, Int J Neuropsychopharmacol 17(10) (2014) 1569-78.

[48] J. Monzon-Sandoval, I. Poggiolini, T. Ilmer, R. Wade-Martins, C. Webber, L. Parkkinen, Human-Specific Transcriptome of Ventral and Dorsal Midbrain Dopamine Neurons, Ann Neurol 87(6) (2020) 853-868.

[49] M. Hamidi, W.C. Drevets, J.L. Price, Glial reduction in amygdala in major depressive disorder is due to oligodendrocytes, Biol Psychiatry 55(6) (2004) 563-9.

[50] C.Y. Pietersen, S.A. Mauney, S.S. Kim, M.P. Lim, R.J. Rooney, J.M. Goldstein, T.L. Petryshen, L.J. Seidman, M.E. Shenton, R.W. McCarley, K.C. Sonntag, T.U. Woo, Molecular profiles of pyramidal neurons in the superior temporal cortex in schizophrenia, J Neurogenet 28(1-2) (2014) 53-69.

[51] W.B. Ruzicka, A. Zhubi, M. Veldic, D.R. Grayson, E. Costa, A. Guidotti, Selective epigenetic alteration of layer I GABAergic neurons isolated from prefrontal cortex of schizophrenia patients using laser-assisted microdissection, Mol Psychiatry 12(4) (2007) 385-97.

[52] A.P. Bannister, Inter- and intra-laminar connections of pyramidal cells in the neocortex, Neurosci Res 53(2) (2005) 95-103.

[53] D. Arion, T. Unger, D.A. Lewis, K. Mirnics, Molecular markers distinguishing supragranular and infragranular layers in the human prefrontal cortex, Eur J Neurosci 25(6) (2007) 1843-54.

[54] D. Arion, S. Horvath, D.A. Lewis, K. Mirnics, Infragranular gene expression disturbances in the prefrontal cortex in schizophrenia: signature of altered neural development?, Neurobiol Dis 37(3) (2010) 738-46.

[55] X. Wu, R. Shukla, K. Alganem, X. Zhang, H.M. Eby, E.A. Devine, E. Depasquale, J. Reigle, M. Simmons, M.K. Hahn, C. Au-Yeung, R. Asgariroozbehani, C.G. Hahn, V. Haroutunian, J. Meller, J. Meador-Woodruff, R.E. McCullumsmith, Transcriptional profile of pyramidal neurons in chronic schizophrenia reveals lamina-specific dysfunction of neuronal immunity, Mol Psychiatry (2021).

[56] J.A. O'Connor, S.E. Hemby, Elevated GRIA1 mRNA expression in Layer II/III and V pyramidal cells of the DLPFC in schizophrenia, Schizophr Res 97(1-3) (2007) 277-88.

[57] J.M. Allman, N.A. Tetreault, A.Y. Hakeem, K.F. Manaye, K. Semendeferi, J.M. Erwin, S. Park, V. Goubert, P.R. Hof, The von Economo neurons in frontoinsular and anterior cingulate cortex in great apes and humans, Brain Struct Funct 214(5-6) (2010) 495-517.

[58] J. Allman, A. Hakeem, K. Watson, Two phylogenetic specializations in the human brain, Neuroscientist 8(4) (2002) 335-46.

[59] C. Butti, M. Santos, N. Uppal, P.R. Hof, Von Economo neurons: clinical and evolutionary perspectives, Cortex 49(1) (2013) 312-26.

[60] L. Yang, Y. Yang, J. Yuan, Y. Sun, J. Dai, B. Su, Transcriptomic Landscape of von Economo Neurons in Human Anterior Cingulate Cortex Revealed by Microdissected-Cell RNA Sequencing, Cereb Cortex 29(2) (2019) 838-851.

[61] A. Kumar, J.R. Gibbs, A. Beilina, A. Dillman, R. Kumaran, D. Trabzuni, M. Ryten, R. Walker, C. Smith, B.J. Traynor, J. Hardy, A.B. Singleton, M.R. Cookson, Age-associated changes in gene expression in human brain and isolated neurons, Neurobiol Aging 34(4) (2013) 1199-209.

[62] C.Y. Pietersen, S.A. Mauney, S.S. Kim, E. Passeri, M.P. Lim, R.J. Rooney, J.M. Goldstein, T.L. Petreyshen, L.J. Seidman, M.E. Shenton, R.W. McCarley, K.C. Sonntag, T.U. Woo,

Molecular profiles of parvalbumin-immunoreactive neurons in the superior temporal cortex in schizophrenia, J Neurogenet 28(1-2) (2014) 70-85.

[63] D.B. Goswami, W.L. May, C.A. Stockmeier, M.C. Austin, Transcriptional expression of serotonergic regulators in laser-captured microdissected dorsal raphe neurons of subjects with major depressive disorder: sex-specific differences, J Neurochem 112(2) (2010) 397-409.

[64] A. Szebeni, K. Szebeni, T. DiPeri, M.J. Chandley, J.D. Crawford, C.A. Stockmeier, G.A. Ordway, Shortened telomere length in white matter oligodendrocytes in major depression: potential role of oxidative stress, Int J Neuropsychopharmacol 17(10) (2014) 1579-89.

[65] G.A. Ordway, A. Szebeni, M.J. Chandley, C.A. Stockmeier, L. Xiang, S.S. Newton, G. Turecki, M.M. Duffourc, M.Y. Zhu, H. Zhu, K. Szebeni, Low gene expression of bone morphogenetic protein 7 in brainstem astrocytes in major depression, Int J Neuropsychopharmacol 15(7) (2012) 855-68.

[66] R. Waller, M.N. Woodroofe, S.B. Wharton, P.G. Ince, S. Francese, P.R. Heath, A. Cudzich-Madry, R.H. Thomas, N. Rounding, B. Sharrack, J.E. Simpson, Gene expression profiling of the astrocyte transcriptome in multiple sclerosis normal appearing white matter reveals a neuroprotective role, J Neuroimmunol 299 (2016) 139-146.

[67] J.J. Bury, A. Chambers, P.R. Heath, P.G. Ince, P.J. Shaw, F.E. Matthews, C. Brayne, J.E. Simpson, S.B. Wharton, F. Cognitive, S. Ageing, Type 2 diabetes mellitus-associated transcriptome alterations in cortical neurones and associated neurovascular unit cells in the ageing brain, Acta Neuropathol Commun 9(1) (2021) 5.

[68] R.E. McCullumsmith, S.M. O'Donovan, J.B. Drummond, F.S. Benesh, M. Simmons, R. Roberts, T. Lauriat, V. Haroutunian, J.H. Meador-Woodruff, Cell-specific abnormalities of glutamate transporters in schizophrenia: sick astrocytes and compensating relay neurons?, Mol Psychiatry 21(6) (2016) 823-30.

[69] I.S. Piras, C. Bleul, I. Schrauwen, J. Talboom, L. Llaci, M.D. De Both, M.A. Naymik, G. Halliday, C. Bettencourt, J.L. Holton, G.E. Serrano, L.I. Sue, T.G. Beach, N. Stefanova, M.J. Huentelman, Transcriptional profiling of multiple system atrophy cerebellar tissue highlights differences between the parkinsonian and cerebellar sub-types of the disease, Acta Neuropathol Commun 8(1) (2020) 76.

[70] S.A. Mauney, C.Y. Pietersen, K.C. Sonntag, T.W. Woo, Differentiation of oligodendrocyte precursors is impaired in the prefrontal cortex in schizophrenia, Schizophr Res 169(1-3) (2015) 374-380.

[71] R. Waller, M.N. Woodroofe, S. Francese, P.R. Heath, S.B. Wharton, P.G. Ince, B. Sharrack, J.E. Simpson, Isolation of enriched glial populations from post-mortem human CNS material by immuno-laser capture microdissection, J Neurosci Methods 208(2) (2012) 108-13.

[72] Y.T. Asi, J.E. Simpson, P.R. Heath, S.B. Wharton, A.J. Lees, T. Revesz, H. Houlden, J.L. Holton, Alpha-synuclein mRNA expression in oligodendrocytes in MSA, Glia 62(6) (2014) 964-70.
[73] J.E. Simpson, S.B. Wharton, P.R. Heath, Immuno-Laser-Capture Microdissection for the Isolation of Enriched Glial Populations from Frozen Post-Mortem Human Brain, Methods Mol Biol 1723 (2018) 273-284.

[74] D. Mastroeni, J. Nolz, S. Sekar, E. Delvaux, G. Serrano, L. Cuyugan, W.S. Liang, T.G. Beach, J. Rogers, P.D. Coleman, Laser-captured microglia in the Alzheimer's and Parkinson's brain reveal unique regional expression profiles and suggest a potential role for hepatitis B in the Alzheimer's brain, Neurobiol Aging 63 (2018) 12-21.

[75] L.W. Harris, M. Wayland, M. Lan, M. Ryan, T. Giger, H. Lockstone, I. Wuethrich, M. Mimmack, L. Wang, M. Kotter, R. Craddock, S. Bahn, The cerebral microvasculature in schizophrenia: a laser capture microdissection study, PLoS One 3(12) (2008) e3964.

[76] B.R. Rocco, H. Oh, R. Shukla, N. Mechawar, E. Sibille, Fluorescence-based cell-specific detection for laser-capture microdissection in human brain, Sci Rep 7(1) (2017) 14213.

[77] F. Wang, J. Flanagan, N. Su, L.C. Wang, S. Bui, A. Nielson, X. Wu, H.T. Vo, X.J. Ma, Y. Luo, RNAscope: a novel in situ RNA analysis platform for formalin-fixed, paraffin-embedded tissues, J Mol Diagn 14(1) (2012) 22-9.

[78] M. Clement-Ziza, D. Gentien, S. Lyonnet, J.P. Thiery, C. Besmond, C. Decraene, Evaluation of methods for amplification of picogram amounts of total RNA for whole genome expression profiling, BMC Genomics 10 (2009) 246.

[79] D. Ramskold, S. Luo, Y.C. Wang, R. Li, Q. Deng, O.R. Faridani, G.A. Daniels, I. Khrebtukova, J.F. Loring, L.C. Laurent, G.P. Schroth, R. Sandberg, Full-length mRNA-Seq from single-cell levels of RNA and individual circulating tumor cells, Nat Biotechnol 30(8) (2012) 777-82.

[80] S. Picelli, O.R. Faridani, A.K. Bjorklund, G. Winberg, S. Sagasser, R. Sandberg, Full-length RNA-seq from single cells using Smart-seq2, Nat Protoc 9(1) (2014) 171-81.

[81] Y.Y. Zhu, E.M. Machleder, A. Chenchik, R. Li, P.D. Siebert, Reverse transcriptase template switching: a SMART approach for full-length cDNA library construction, Biotechniques 30(4) (2001) 892-7.

[82] A. Chenchik, L. Diachenko, F. Moqadam, V. Tarabykin, S. Lukyanov, P.D. Siebert, Full-length cDNA cloning and determination of mRNA 5' and 3' ends by amplification of adaptor-ligated cDNA, Biotechniques 21(3) (1996) 526-34.

[83] J. Wilhelm, J.P. Muyal, J. Best, G. Kwapiszewska, M.M. Stein, W. Seeger, R.M. Bohle, L. Fink, Systematic comparison of the T7-IVT and SMART-based RNA preamplification techniques for DNA microarray experiments, Clin Chem 52(6) (2006) 1161-7.

[84] J.E. Lang, M.J. Magbanua, J.H. Scott, G.M. Makrigiorgos, G. Wang, S. Federman, L.J. Esserman, J.W. Park, C.M. Haqq, A comparison of RNA amplification techniques at sub-nanogram input concentration, BMC Genomics 10 (2009) 326.

[85] Z. Wang, M. Gerstein, M. Snyder, RNA-Seq: a revolutionary tool for transcriptomics, Nat Rev Genet 10(1) (2009) 57-63.

Figure 1

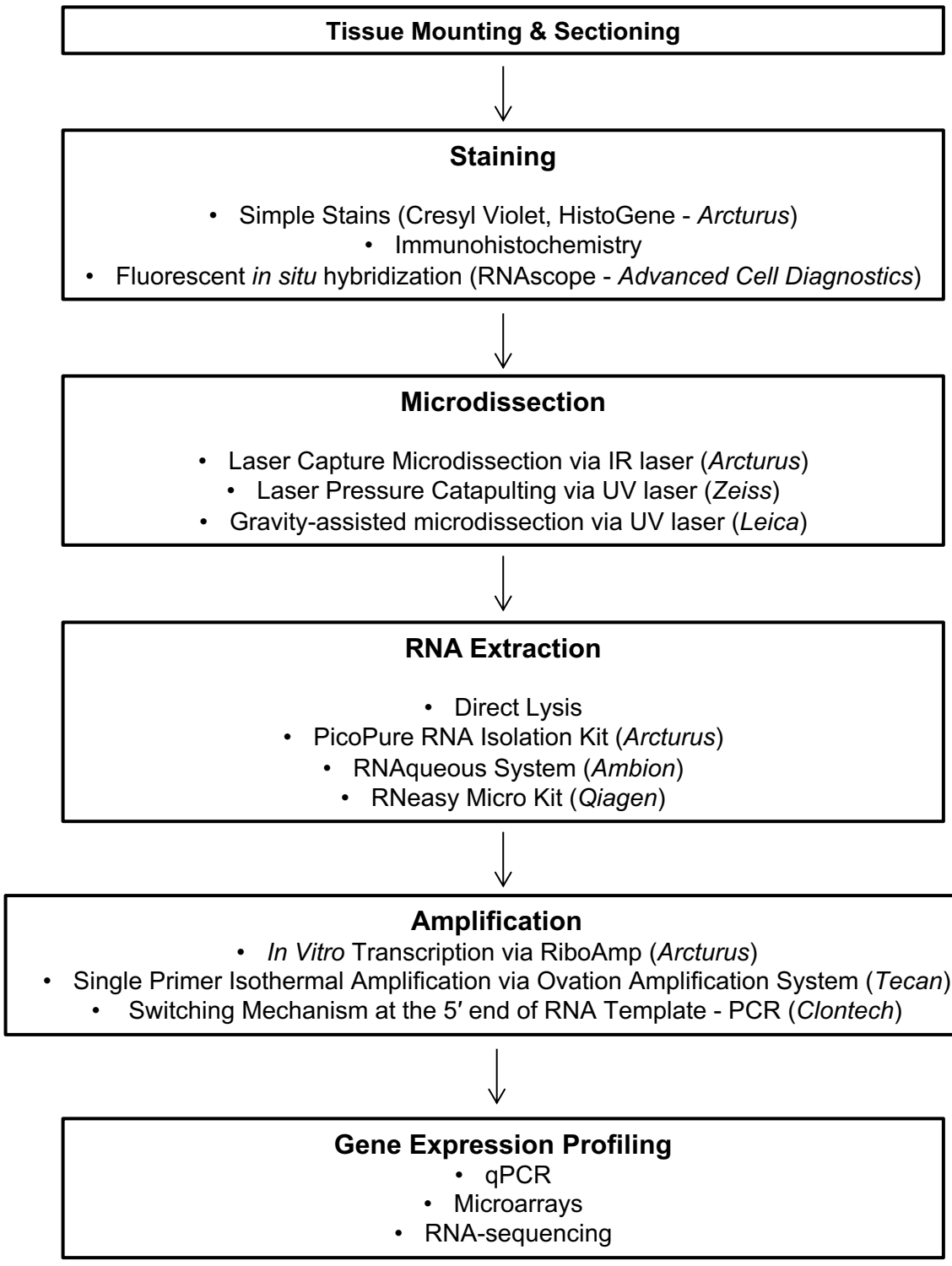
Tissue Mounting & Sectioning
Staining
• Simple Stains (Cresyl Violet, HistoGene - *Arcturus*)
• Immunohistochemistry
• Fluorescent *in situ* hybridization (RNAscope - *Advanced Cell Diagnostics*)
Microdissection
• Laser Capture Microdissection via IR laser (*Arcturus*)
• Laser Pressure Catapulting via UV laser (*Zeiss*)
• Gravity-assisted microdissection via UV laser (*Leica*)
RNA Extraction
• Direct Lysis
• PicoPure RNA Isolation Kit (*Arcturus*)
• RNAqueous System (*Ambion*)
• RNeasy Micro Kit (*Qiagen*)
Amplification
• *In Vitro* Transcription via RiboAmp (*Arcturus*)
• Single Primer Isothermal Amplification via Ovation Amplification System (*Tecan*)
• Switching Mechanism at the 5′ end of RNA Template - PCR (*Clontech*)
Gene Expression Profiling
• qPCR
• Microarrays
• RNA-sequencing

Table 1

Citation	Cell-type or Sub-region	Staining Procedure	RNA extraction	cDNA synthesis or Amplification	Downstream approach
Mojsilovic-Petrovic et al., 2004	Microvessels	Fluorescein-labeled Ulex Europeaus Agglutinin I	Absolutely RNA Microprep Kit	SuperScript RT II	End-point PCR
Arion et al., 2007	Layers II – III & layers V – VI of the PFC	Cresyl violet	RNAqueous micro kit	Ovation linear amplification system	Affymetrix GeneChip HG-U133A Array
O'Connor et al., 2007	Layers II – II & layer V pyramidal neurons of the PFC	Cresyl violet	PicoPure RNA isolation kit	SuperScript RT III	qPCR
Ruzicka et al., 2007	Layer I GABAergic interneurons & layer V pyramidal neurons of the PFC	Toluidine blue	RNeasy Micro kit	Not described	Nested competitive RT-PCR
Harris et al., 2008	Pyramidal neurons & microvessel endothelial cells	anti-Neurofilament & anti-von Willebrand factor antibodies	PALM RNA extraction kit	RNA amplification via RiboAmp HS kit	Affymetrix GeneChip HG-U133 Plus 2.0 Array
Bernard et al., 2009	SERT & NET+ cells used to define the boundaries of the DR, MR and LC	Radioactive *in situ* hybridization	PicoPure RNA isolation kit	RNA amplification via RiboAmp kit	Affymetrix GeneChip HG-U133 Plus 2.0 Array
Ordway et al., 2009	Astrocytes, oligodendrocytes & noradrenergic neurons	Histogene staining kit, modified Cresyl violet & anti-GFAP antibody	RNAqueous micro kit	SuperScript III platinum transcriptase kit	End-point PCR
Slevin et al., 2009	Active and inactive microvessel-rich regions from stroke affected patients	anti-CD31, anti-CD105 & anti-FLT1 antibodies	RNeasy Micro kit	Not described	qPCR
Arion et al., 2010	Layers II – III & layers V – VI of the PFC	Cresyl violet	RNAqueous micro kit	Ovation linear amplification system	Affymetrix GeneChip HG-U133 Plus Array
Goswami et al., 2010	Serotonergic neurons	anti-TPH2 antibody	PicoPure RNA isolation kit	Sensiscript RT kit	qPCR
Katsel et al., 2011	Layers II – III, layers IV – VI & white matter of the ACC	Thionin	PicoPure RNA isolation kit	Not described	qPCR
Kerman et al., 2012	SERT+ cells used to define the boundaries of the DR	Klüver–Barrera method & radioactive *in situ* hybridization	PicoPure RNA isolation kit	RNA amplification via RiboAmp OA kit	Affymetrix GeneChip HG-U133 Plus 2.0 Array
Waller et al., 2012	Astrocytes, oligodendrocytes & microglia	anti-GFAP, anti-CD68 & anti-OSP antibodies	PicoPure RNA isolation kit	qScript cDNA supermix	End-point PCR

Kumar et al., 2013	Purkinje cells	Cresyl violet	PicoPure RNA isolation kit	RNA amplification via MessageAmp II aRNA kit	Illumina HumanHT-12 v3 Expression BeadChip
Asi et al., 2014	Neurons & oligodendrocytes	Toluidine blue & anti-OSP antibody	PicoPure RNA isolation kit	SuperScript VILO cDNA synthesis kit	qPCR
Chandley et al., 2014	Noradrenergic & pyramidal neurons	Histogene staining kit	RNAqueous system	SuperScript III	End-point PCR
Pietersen et al., 2014	Layer III pyramidal neurons of the STG	Histogene staining kit	PicoPure RNA isolation kit	RNA amplification via RiboAmp kit	Affymetrix GeneChip Human X3P Array
Pietersen et al., 2014	PV+ GABAergic interneurons	anti-PV antibody	PicoPure RNA isolation kit	RNA amplification via RiboAmp kit	Affymetrix GeneChip Human X3P Array
Szebeni et al., 2014	Astrocytes & oligodendrocytes	anti-GFAP & anti-CNP antibodies	RNAqueous micro kit	SuperScript III platinum transcriptase kit	End-point PCR
Arion et al., 2015	Layer III & layer V pyramidal neurons of the PFC	Thionin	RNeasy Plus Micro kit	Ovation Pico WTA	Affymetrix GeneChip HG-U133 Plus Array
Mauney et al., 2015	Oligodendrocyte precursor cells	anti-CNP antibody	PicoPure RNA isolation kit	RNA amplification via RiboAmp kit	Affymetrix GeneChip Human X3P Array
McCullumsmith et al., 2016	Glutamatergic relay neurons & astrocytes	Cresyl violet	PicoPure RNA isolation kit	High-capacity cDNA Reverse Transcription Kit	qPCR
Medina et al., 2016	*MR+ cells used to define the boundaries of the hippocampus	*In situ* hybridization	PicoPure RNA isolation kit	RNA amplification via RiboAmp Plus kit	Illumina HumanHT-12 v4 Array
Nichterwitz et al., 2016	Dopaminergic neurons	Histogene staining kit & anti-TH antibody	Direct lysis without RNA extraction	SMART-seq2	RNA-seq
Tagliafierro et al., 2016	Neurons & astrocytes	anti-Neurofilament & anti-GFAP antibodies	RNAqueous micro kit	SuperScript VILO cDNA synthesis kit	nCounter Single Cell Gene Expression Assay
Waller et al., 2016	Astrocytes	anti-GFAP antibody	PicoPure RNA isolation kit	GeneChip 3′ IVT Express amplification protocol	Affymetrix GeneChip HG-U133 Plus 2.0 Array
Rocco et al., 2017	SLC17A7+ excitatory neurons & SST+ inhibitory interneurons	Fluorescent *in situ* hybridization via RNAscope	PicoPure RNA isolation kit	SuperScript VILO cDNA synthesis kit	qPCR

Mastroeni et al., 2018	Activated microglia	anti-LN3	RNeasy Micro kit	Ovation RNA-Seq System v2	RNA-seq
Yang et al., 2019	von Economo neurons & pyramidal neurons	Cresyl violet	Direct lysis without RNA extraction	Previously published protocol	RNA-seq
Jaffe et al., 2020	Granule cell layer of the dentate gyrus	Nucleic acid-intercalating agent Acridine Orange	RNeasy Micro kit	Illumina RiboZero Gold library	RNA-seq
Monzon-Sandoval et al., 2020	Dopaminergic neurons	Cresyl violet	PicoPure RNA isolation kit	SMARTer Kit	RNA-seq
Piras et al., 2020	Oligodendrocytes	Modified H&E	PicoPure RNA isolation kit	SMARTer Stranded Total RNA-Seq Kit - Pico Input for cDNA synthesis and Illumina library prep	RNA-seq
Bury et al., 2021	Cortical neurons, astrocytes & microvessel endothelial cells	Toluidine blue, anti-GFAP & anti-collagen IV antibodies	PicoPure RNA isolation kit	GeneChip 3′ IVT Pico Kit	Affymetrix GeneChip HG-U133 Plus 2.0 Array
Wu et al., 2021	Layers II – III and layers IV – VI pyramidal neurons	Cresyl violet	QuickGene RNA Tissue kit	Ovation Pico WTA	Affymetrix GeneChip Human Gene 1.0 ST Arrays

Abbreviations: CD105 = cluster of differentiation 105, CD31 = cluster of differentiation 31, CD68 = cluster of differentiation 68, CNP = 2',3'-Cyclic Nucleotide 3' Phosphodiesterase, DR = dorsal raphe, FLT1 = Fms Related Receptor Tyrosine Kinase 1, GFAP = glial fibrillary acidic protein, LC = locus coeruleus, LN3 = anti-HLA-DR, MR = median raphe, *MR = mineralocorticoid receptor, NET = norepinephrine transporter, OSP = Oligodendrocyte-Specific Protein, PFC = prefrontal cortex, PV = parvalbumin, SERT = serotonin transporter, SLC17A7 = Solute Carrier Family 17 Member 7, SST = somatostatin, STG = superior temporal gyrus, TH = tyrosine hydroxylase, TPH2 = tryptophan hydroxylase 2